ON A DESIGN METHOD OF COMPOSITES STEM BASED ON CT IMAGES

Takeshi KAWAMURA*, Masaru ZAKO, Tetsusei KURASHIKI**, Hiroaki NAKAI**, Takafumi FURUTA*, Nobuhiko SUGANO***, Hideki YOSHIKAWA*** and Shun'ichi BANDOH******

***Graduate Student of Osaka University, **Graduate School of Engineering, Osaka University, ***Graduate School of Medicine, Osaka University, ****B. I. TEC Co. Ltd.**

Keywords: *CT Images, Stem, Composites, FEM, Simplified-model, Linear Mapping, Basic Design*

Abstract

Although a tailor-made stem using composites is proposed as an advanced prosthesis, it is not easy to determine the design parameters like thickness, fiber orientation etc. because of its complex shape and anisotropic properties.

The purpose of this study is to establish a design method of composites stem. A 'Simplified-model' of stem and femur is proposed as a basic design tool. The Simplified-model is correlated with 'Real-model': acquired from CT images of a patient, by linear mapping matrixes calculated by correspondence of the shape of Simplified and Real-models. The analytical results and responses to design parameters of Simplified and Real-model are compared and discussed. A composites stem is fabricated and the estimation about composites stem is verified by in-vitro test using a composites and a metal stems.

1 Introduction

The number of patient of bone fracture is increasing year after year, e.g. there are 1.3 ~ 1.7 million hip fracture patients at 1990 in the world, and it is estimated that the number of patients will be 3 million until 2025 [1]. Total Hip Replacement (THR) is an effective remedy for serious hip-diseases. Fig. 1 shows the typical examples of X-ray images of hip disease patient. Although THR is a conventional treatment, the lack of mechanical biocompatibility of the stem is a serious problem because its high rigidity causes 'stress shielding' which suppresses bone remodeling [2, 3].

Composites attract many attentions as an alternate material to metal for stem. A tailor-made composites stem could be possible to reduce the stress shielding because the rigidity could be treated as a design parameter. Fig. 2 shows a schematic drawing of composites stem and a picture of fabricated prototype. It had indicated that the composites stem is able to reduce stress shielding from a result of numerical analysis [4]. Although the composites stem is beneficial, the design of the composites stem is more difficult than a traditional metal stem.

(a) preoperative (b) postoperative

Fig. 1. Typical examples of X-ray image of hip-joint

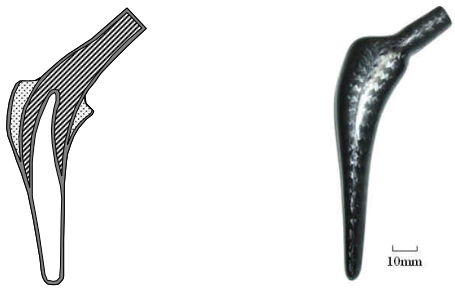

(a) Schematic drawing (b) Prototype

Fig. 2. Composites stem

The purpose of this study is to establish a design method for composites stem. In this paper, a design method using Simplified-model and Real-model is proposed. The concept and the modeling method of femur are described. Finite element analyses are carried out in two models and the results are discussed. Finally, the analytical

estimation is verified by in-vitro tests for composites and metal stems.

2 Design and Modeling Method

2.1 Modeling of Real-model based on CT Images

A three dimensional geometry of femur must be modeled for designing a stem which has a compatible outer shape. It is a practical method to acquire the geometry of femur from CT images of the patient. The geometry of femur is applied to design the outer-shape of stem [5]. Fig. 3 shows a procedure of making Real-model of a patient.

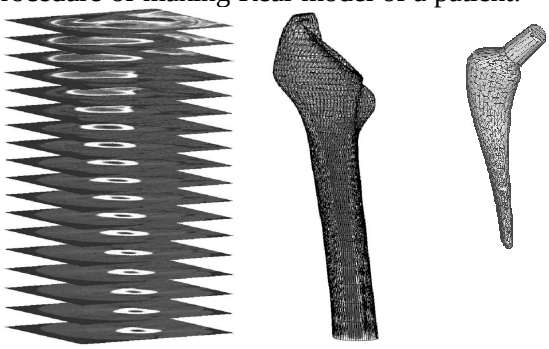

(a) CT images (b) Femur geometry (c) Designed outer shape of stem

Fig. 3. A procedure of making Real-model

In the case of 'uncemented stem', the 'Fit' and 'Filling' are important evaluation indices for shape design of stem. 'Fit' is the percentage of surface area of the implant in direct contact with the endosteal surface, and 'Filling' is the percentage of the cross-sectional area of the femoral canal occupied by the prosthesis [6]. High percentages of fit and filling are desired. According to Nishihara and Sugano et al. [7], these parameters of fit and filling for metal stem are 5 ~ 40 % and 35 ~ 85 %, respectively. In order to make higher percentage, the suitable shape stem has to be considered and designed. Because of the lack of the shape compatibility of a stem, the load transfer mechanism from stem to femur makes very complex and difficult.

2.2 Modeling of Simplified-model

A 'Simplified-model' as shown in Fig. 4 has been proposed for briefly investigation of design the inner structure of composites stem. Simplified-model has a hollow cylindrical shape and the interfaces between stem and femur is completely connected so that the loads are transferred from stem to femur ideally. A cementless stem was modeled by simulating the long term secured state where the bone at the bone and stem interface was grown well to simulate the stress shielding in the long term.

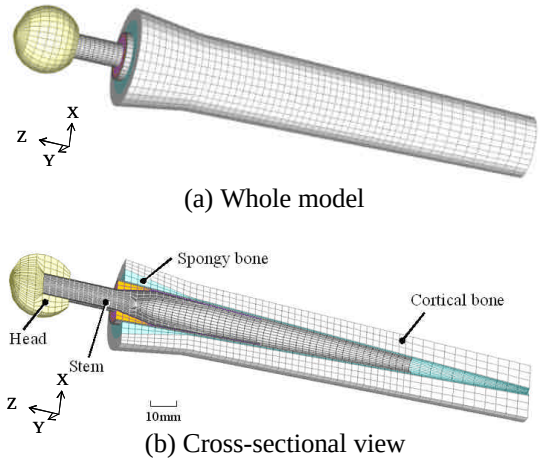

(a) Whole model

(b) Cross-sectional view

Fig.4. An example of Simplified-model

It is a key point that the distributions of cross-sectional area in Simplified-model are approximately same in each lengthwise position. In other word, the modulus of section of Simplified-model is approximately same order as that of Real-model. Therefore, compressive and torsional rigidity of the both models are approximately same. Fig. 5 shows an example of distributions of cross-sectional area of Simplified-model and two Real-models made from CT images of two patients.

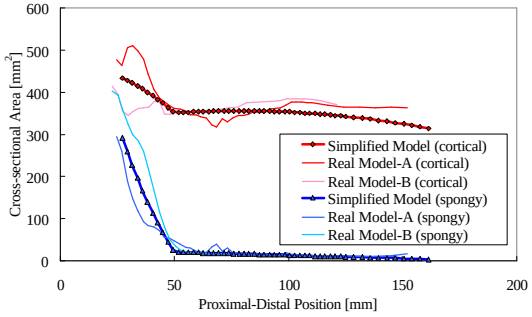

(a) Cortical and spongy bone of femur

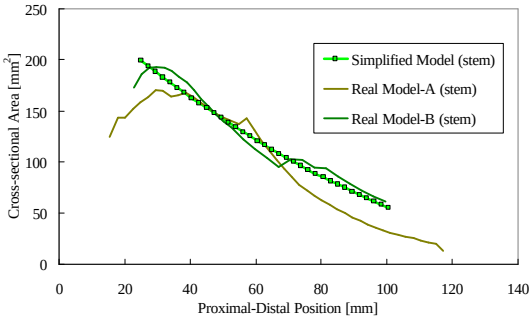

(b) Outer shape of stem

Fig.5. An example of cross-sectional area distribution of Simplified and Real-models

In order to set same stiffness to the Simplified and Real-models, the mechanical properties must be same in each position.

It has been reported that the mechanical properties of bone can be measured by bone density [8-13], and bone density has been acquired by Quantitative Computed Tomography (QCT) [14]. According to the proposed method, the mechanical properties of bone are able to be estimated by QCT imaging and image processing. The images in this paper are not QCT, we refer only the distribution of CT value in lengthwise direction and assume the relationship of CT value and mechanical properties of bone from a practical point of view.

Fig. 6 shows distributions of CT value acquired from two image sets in lengthwise direction. The unit of CT value 'hu' represents the relative X-ray absorb coefficient. The coefficient of water and air is defined as 0hu and -1000hu, respectively. Generally the CT value of cortical bone is about 400~hu and of spongy bone is about 0 ~ 400hu. On the other hand, the order of Young's modulus of cortical bone is about 10 ~ 20GPa and of spongy bone is about ~150MPa. We assume a relationship between CT value and Young's modulus. Examples of CT value distributions are shown in Fig. 6. Poisson's ratio is assumed as constantly 0.3 because of an experimental result of the relationship between bone density and Poisson's ratio [12].

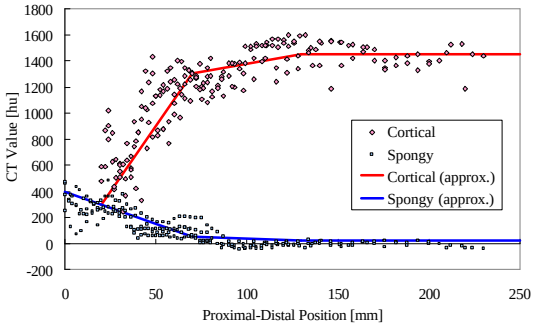

Fig.6. Examples of CT value distribution from two image sets of patients

The design parameters of composites stem, e.g. thickness of lamina, fiber orientation, stacking pattern etc., are determined quantitatively on Simplified-model by finite element model and the mechanical propertied.

2.3 Model Conversion by Linear Mapping

After the determination of design parameter of Simplified-model for a patient, the design parameters of Real-model can be determined. We describe the methodology how to reflect the design parameters on Simplified-model to on Real-model.

The difference of Simplified and Real-model is the shape. If the correlation between Simplified and Real-model is defined, the design parameters will be able to convert as follows.

First, the boundaries on each cross-section in Simplified and Real-models are defined. Typical examples of boundaries and cross-sections are shown in Fig.7, and a schematic drawing of boundaries is shown in Fig. 8.

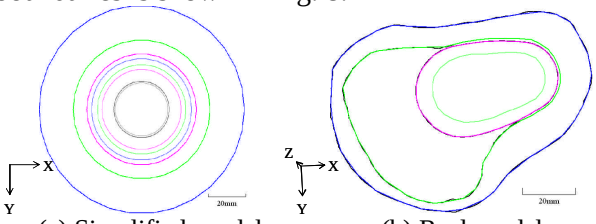

(a) Simplified-model (b) Real-model

Fig.7. Cross-sections and boundaries for each model

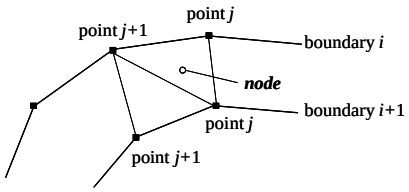

Fig.8. Schematic drawing of geometric correlation

Next, a discrete linear mapping matrix is calculated based on the correlation and regions. The node coordinate is mapping by below equation.

$$\{\mathbf{p}^{r}_{node}\} = [\mathbf{R}][\mathbf{S}]^{-1}\{\mathbf{p}^{s}_{node}\}, \quad (1)$$

$$[\mathbf{R}] = \left[\{\mathbf{p}^{r}_{i,j}\} \quad \{\mathbf{p}^{r}_{i,j+1}\} \quad \{\mathbf{p}^{r}_{i+1,j}\}\right],$$

$$[\mathbf{S}] = \left[\{\mathbf{p}^{s}_{i,j}\} \quad \{\mathbf{p}^{s}_{i,j+1}\} \quad \{\mathbf{p}^{s}_{i+1,j}\}\right],$$

$$\{\mathbf{p}\} = \{p_x \quad p_y \quad p_z\}^T,$$

where vector **{p}** represents a coordinate of a node or a point of geometry, suffix *s* and *r* represent the model, matrix **[S]** and **[R]** represent a mapping matrix calculated by three points of each region in Simplified and Real-model, suffix *i* and *j* represent boundary number and point number in a boundary, respectively. Applying this procedure to all nodes of a Simplified-model, a Real-model is acquired. An example of model conversion is shown in Fig. 9.

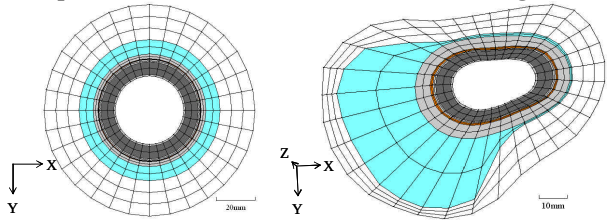

(a) Simplified-model (b) Real-model

Fig.9. Model Conversion

The flowchart of the proposed model conversion procedure written in above is shown in Fig. 10.

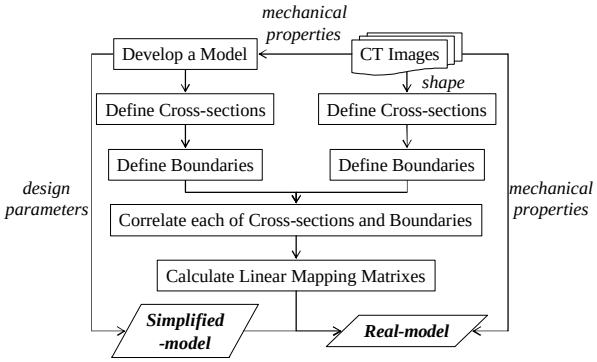

Fig. 10. Flowchart of Model Conversion

3 Basic Design of Composites Stem

3.1 Design Parameters

The proposed composites stem is consisted of two components. One is 'main spar' which bears vertical and bending load, and the other is 'outer skin' which bears torsional loads. The material for the stem is carbon fiber reinforced poly-ether-ether-ketone (CF/PEEK) which has biocompatibility.

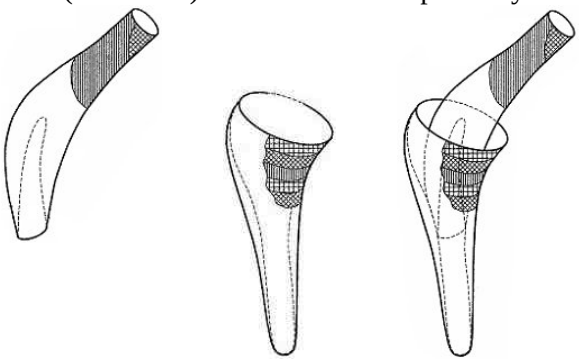

(a) Main spar (b) Outer skin (c) Whole

Fig. 11. Schematic drawings of proposed composites stem

Main spar is mainly consisted of uni-directional (UD) CF/PEEK which has high compressive and bending rigidity, and outer skin is molded by cloth or fabric CF/PEEK which has high torsional rigidity. Rigidities of a stem are able to design individually by changing the taper length (thickness of laminate) or the stacking pattern of each component [4].

Mechanical properties of composites and other isotropic materials for finite element analysis are shown in Table 1.

Table 1 Mechanical properties

Constants		*CFRP (UD)*	*Ti-6Al-4V (Metal Stem)*	*PEEK (Resin)*	*ZrO_2 (Head)*
E [GPa]	*l*	150	126	4	255
	t	9.81			
	z	9.81			
G [GPa]	*tz*	1.43	49.6	1.3	98.1
	zl	5.49			
	lt	5.49			
n	*tz*	0.4	0.27	0.4	0.3
	zl	0.022			
	lt	0.34			

3.2 Design Examples of Composites Stem

3.2.1 Main Spar

Three types of composites stem (short, middle, and long type) which have different length of main spar are designed. These stems have different cross-sectional area at each section in the lengthwise direction, too. *EA* (compressive rigidity), GI_p (torsional rigidity) are compared, because each stem has different rigidities. *E* and *G* represent Young's modulus and shear modulus, *A* represents cross-sectional area and I_p represents polar moment of inertia of cross-sectional area, respectively. I_p is calculated by below equation.

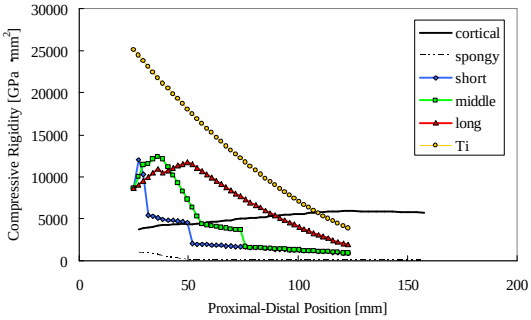

(a) Distribution of *EA* (compressive rigidity)

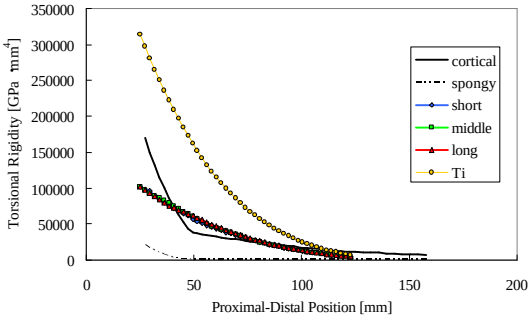

(b) Distribution of GI_p (torsional rigidity)

Fig.12. Distributions of rigidity in Simplified-model (the case of changing main spar)

$$I_p = \frac{p\left(d_2{}^4 - d_1{}^4\right)}{32} \quad (2)$$

where d_1 and d_2 represents inner and outer diameter, respectively.

Distributions of EA and GI_p of a femur for three composites stem, and for a traditional metal stem (Ti) are shown in Fig. 12. Each stem has the same outer shape. Three composites stems with different EA and same GI_p can be designed, because E and G of composites are able to be designed independently. From Fig. 12, it is recognized that Ti stem has higher rigidity than composites stem.

3.2.2 Outer Skin

Three types of composites stem (low, middle, and high type) which has different shear modulus of outer skin are designed. In this paper, a plane woven fabric is assumed as the material of outer skin. The mechanical properties like E_l and G_{lt} can be changed by the rotation in plane or the choice of fiber of woven cloth. In this paper, three types of fiber bundles which have different E_l were chosen. The properties are shown in Table 2. Distributions of rigidity of a femur, composites stems, and a metal stem are shown in Fig. 13. The three composites stems have same EA and different GI_p.

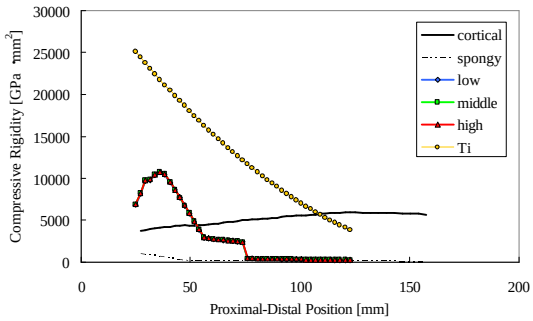

(a) Distribution of EA (compressive rigidity)

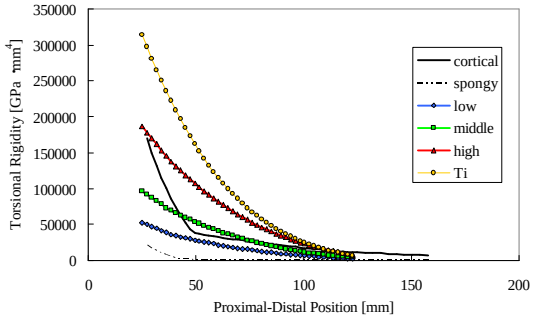

(b) Distribution of GI_p (torsional rigidity)

Fig.13. Distributions of rigidity in Simplified-model (the case of changing outer skin)

Table 2 Mechanical properties of outer skin

Constants		CFRP (low)	CFRP (middle)	CFRP (high)
E [GPa]	l	58.5	117	234
	t	58.5	117	234
	z	9.8	9.8	9.8
G [GPa]	tz	5.49	5.49	5.49
	zl	5.49	5.49	5.49
	lt	6.08	6.08	6.08
n	tz	0.34	0.34	0.34
	zl	0.057	0.029	0.014
	lt	0.05	0.05	0.05

3.3 Analysis and Evaluation Method

Five composites stems and one metal stem were compared. A verified finite element code SACOM which had been developed by authors [15] was used in this study. An isotropic hexahedral element with eight nodes was applied in the solver.

3.3.1 Boundary Conditions

Compressive and torsional loads are applied at a head of Simplified-model. The distal tip of Simplified-model is constrained in three directions.

Local coordinate systems are defined in each element for two reasons. One is for definition of material coordinate system of orthotropic materials. The other is for transforming coordinate systems of analytical results for evaluation.

Schematic drawing of boundary conditions and defined local coordinate systems is shown in Fig. 14.

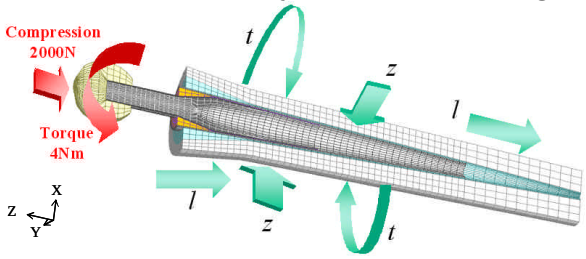

Fig. 14. Boundary condition and local coordinate systems in Simplified-model

3.3.2 Evaluation Indices

Two evaluation indices are used in this paper. One is Strain Energy Density (SED) as a index of stress shielding, the other is shear stress in lengthwise and torsional directions as a index of securing position.

Stress shielding is able to be evaluated by SED, because it is reported that SED is an influential factor of bone remodeling phenomenon [16, 17]. Therefore, a high SED at the femur suppresses stress shielding and promotes bone remodeling, while a small SED promotes stress shielding and suppresses

bone remodeling. SED $U(e_l, e_t, \cdots, g_{lt})$ is calculated from analytical result by below equation.

$$U(e_l, e_t, \cdots, g_{lt}) = \frac{1}{2}\{e_L\}^T[\mathrm{D}]\{e_L\} = \frac{1}{2}\{e_L\}^T\{s_L\} \quad (3)$$

$$\{e_L\}^T = [e_l \quad e_t \quad e_z \quad g_{tz} \quad g_{zl} \quad g_{lt}]$$

$$\{s_L\}^T = [s_l \quad s_t \quad s_z \quad t_{tz} \quad t_{zl} \quad t_{lt}]$$

where $\{e_L\}$ is strain vector, $\{s_L\}$ is stress vector, [D] is stress-strain matrix, respectively.

A securing position on model is used to evaluate whether the loads are transferred proximally or distally. Load is transferred from hip joint to femur through stem, it is believed that the load transferred positions can be evaluated by using shear stresses on the spongy bone where a stem contacts to a femur. The definition of local coordinate system is shown in Fig. 14. We have reported that and proximal securing is preferable [4], t_{zl} and t_{tz} is used for indices in lengthwise and torsional directions.

These two indices are calculated by finite element analyses.

3.4 Finite Element Analyses of Simplified-model

SED distributions on the cortical bone are shown in Fig. 15. The horizontal axis indicates the position in the lengthwise direction of femur, i.e. left side represents the proximal part on femur and right side represents the distal part on femur, respectively. As shown in Fig. 15, SED of composite stems are higher than a metal stem. Therefore, it is recognized that the composite stem will reduce stress shielding compared to metal stem. Comparing the two design cases, the effect of main spar is larger than the effect of outer skin, because large varies of distribution of SED is observed in Fig. 15 (a) and few varies is observed in (b). Therefore, it is revealed that a main spar is a sensitive design parameter to stress shielding of femur. A low rigidity stem suppresses stress shielding and promotes bone remodeling while a high rigidity stem promotes stress shielding and suppresses bone remodeling.

t_{zl} and t_{tz} distributions in spongy bone are shown in Fig. 16 and 17. It is observed that a metal stem produces higher shear stresses at the tip of stem (120mm position) than composites stems. Since load from the stem to the femur is mainly transferred in a region of great shear stress, the metal stem indicates a remarkable load transfer at the distal part of femur: distal securing. On the other hand, composites stems produce smaller shear stresses at the distal part of the femur but greater shear stresses at the proximal part instead. Therefore, the composites stem is superior to the metal stem in terms of proximal securing.

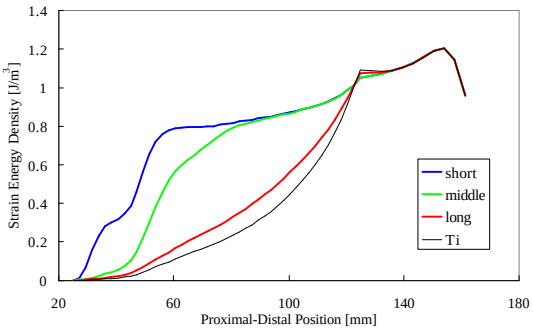

(a) The case of changing main spar

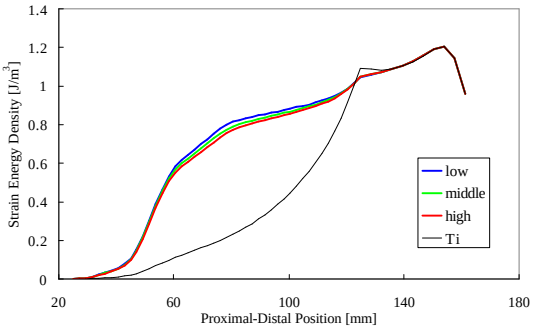

(b) The case of changing outer skin

Fig.15. Distributions of SED in cortical bone, Simplified-model

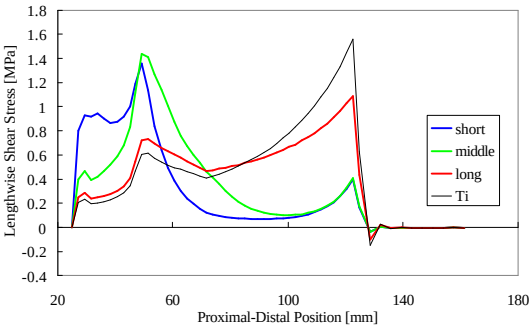

(a) The case of changing main spar

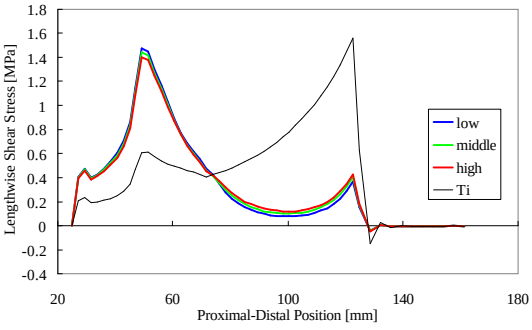

(b) The case of changing outer skin

Fig.16. Distributions of t_{zl} in spongy bone, Simplified-model

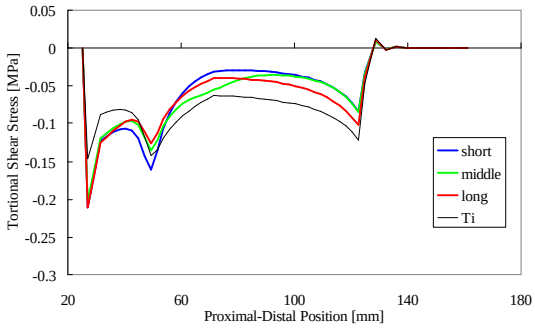

(a) The case of changing main spar

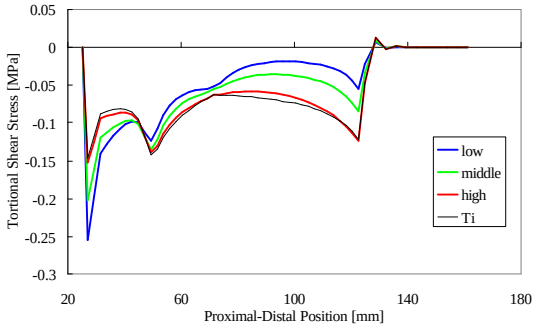

(b) The case of changing outer skin

Fig.17. Distributions of t_{tz} in spongy bone, Simplified-model

Comparing the results of composites stems, it is observed that t_{zl} distribution is changed significantly by main spar but is not changed completely by outer skin. It is also observed that t_{tz} distribution is changed small by main spar but is changed significantly by outer skin. From these results, it became clear that the securing positions in lengthwise and torsional direction are able to be designed independently by changing the design of main spar and outer skin. In other words, each design parameter does not affect each other.
It is recognized that the several distributions of stress can be selected by changing the design parameters of stem.

4 Confirmation of Basic Design

The relationship of analytical results between Simplified and Real-model must be verified. In this chapter, analytical results of Real-model are compared with results of Simplified-model.

4.1 Modeling and Analysis of Real-model

Simplified-model has been converted by the procedure described in 2.3. Models before and after conversion are shown in Fig. 18.

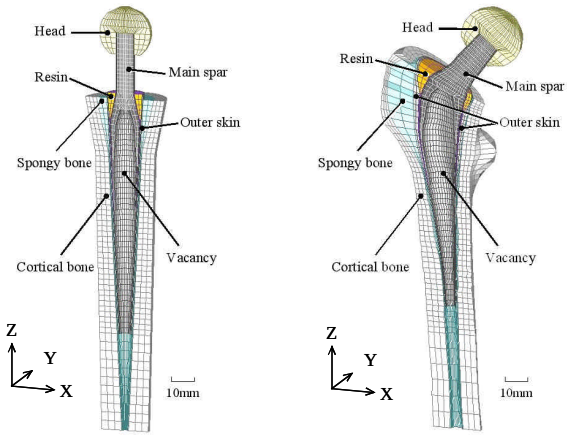

(a) Before conversion (Simplified-model) (b) After conversion (Real-model)

Fig.18. Cross-sectional view of models

Although a femur has various muscles, the load conditions are determined as shown in Fig. 19 (a) by considering the muscular tension of the abductors only [18]. This is a reason why the stress shielding at a lateral femur is overestimated if abductors are not considered [19]. The end of the femur has been totally constrained [18].

Local coordinate systems are defined for each element of the analytical model. Regarding the major directions of coordinate systems, the lengthwise direction of a femur and a stem is defined as *l*, the circumferential direction as *t*, and the radial direction as *z*. Fig. 19 (b) is a schematic drawing of the major directions.

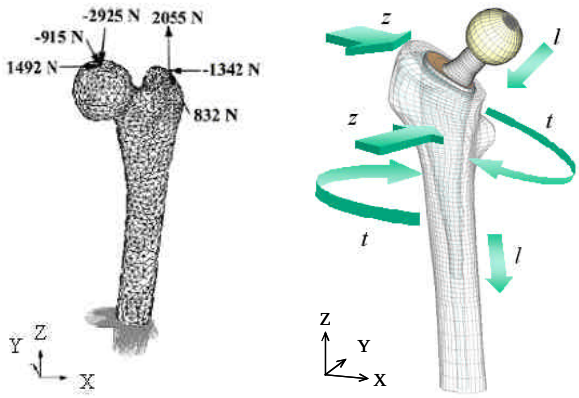

(a) Load conditions [18] (b) Definition of material coordinate system

Fig.19. Boundary condition and local coordinate systems in Real-model

4.2 Comparison of the Results

SED, t_{zl} and t_{tz} and distribution on the cortical bone in Real-model is shown in Figs. 20, 21 and 22. Distributions at medial femur are described.

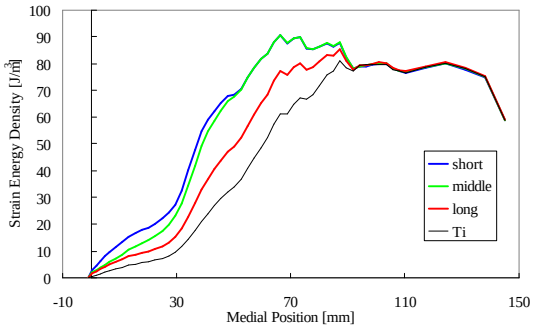

(a) The case of changing main spar

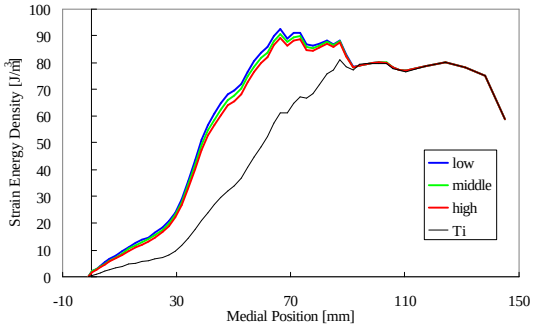

(b) The case of changing outer skin

Fig.20. Distributions of SED in cortical bone, Real-model

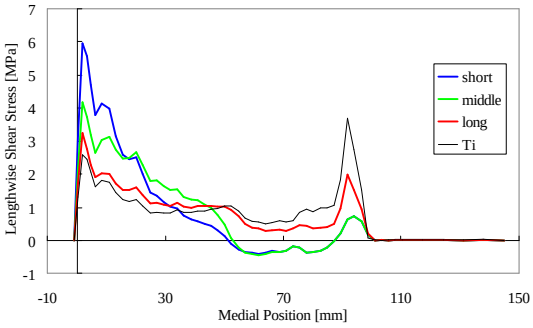

(a) The case of changing main spar

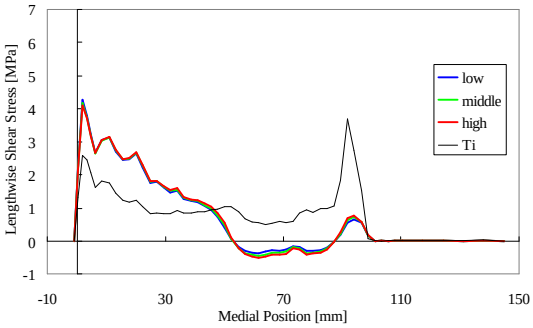

(b) The case of changing outer skin

Fig.21. Distributions of t_{zl} in spongy bone, Real-model

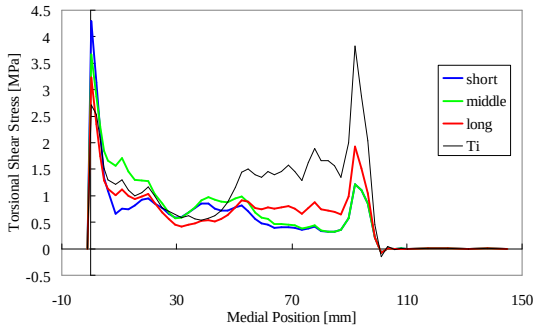

(a) The case of changing main spar

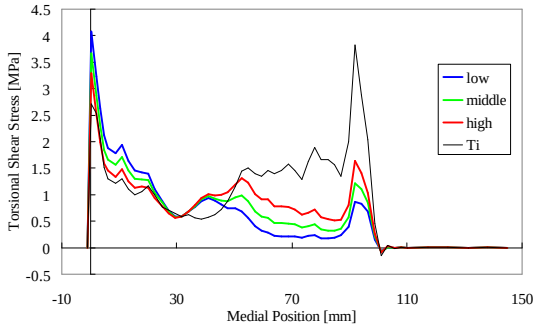

(b) The case of changing outer skin

Fig.22. Distributions of t_{tz} in spongy bone, Real-model

Although the distributions are not smooth curve, there are approximately same tendencies to the results of Simplified-model as shown in Figs. 15, 16 and 17. It is recognized for middle and short types that the sign of t_{zl} turns negative at distal region (about 50 ~ 90mm in horizontal axis) from Fig. 21. These phenomena are generated by the moment, which the stem tears from the bone by the small rigidity of distal part of stem. As the result, the responses of the Simplified-model have good correlations with the result of Real-model. Therefore, it became clear that a basic design of composites stem is possible by using Simplified-model and it has beneficial effects for rigidity design of composite stem which has complex shape and structure.

5 Verification of Concept of Composites Stem

5.1 Fabrication of a Composites Stem

A composites stem for a dried real femur (a desiccated dead femur) is designed from the knowledge of basic design method, and it has been fabricated. It was tested mechanically and compared with a metal stem which has the same outer shape. The fabricated composites stem and metal stem is shown in Fig. 23.

(a) Fabricated composites stem (CF/PEEK)

(b) Metal stem (Ti-6Al-4V)

Fig.23. Tested stems

5.2 Test Apparatus

In-vitro compression test has been performed on a dynamic servo-hydraulic testing machine (Shimadzu Servopulser EHF-LB10kN-4LA). Rosette gauges are put on the dried femur. The specimen holder is designed to enable to set specimen at any angle in order to carry out tests under the different loading angles. The actuator has a moving unit to release transversal loads to the load cell. Dial gauge is set at the side of the actuator to measure the displacement of moving unit. Fig. 24 shows the in-vitro testing apparatus.

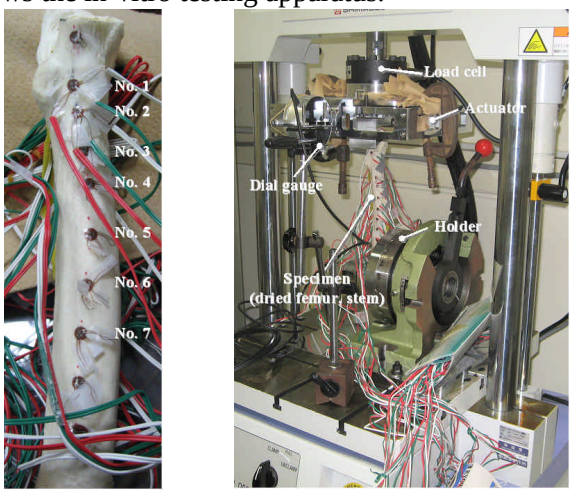

(a) Gauges on dried femur (medial)

(b) Test setup

Fig.24. In-vitro test apparatus

5.3 Results and Discussions

Compressive load is applied to the head of stem by displacement control. Each stem are inserted to the dried femur and -0.6mm displacement is applied to the head and strain is measured by rosette gauges. Measured strains are normalized by the maximum load.

The minimum principal strains normalized by load on the medial femur are shown in Fig. 25. The composites stem produces higher strain than the metal stem at all gauges. It reveals that composites stem produces larger mechanical energy than metal stem. This is the same tendency to the results of analytical investigation as mentioned before.

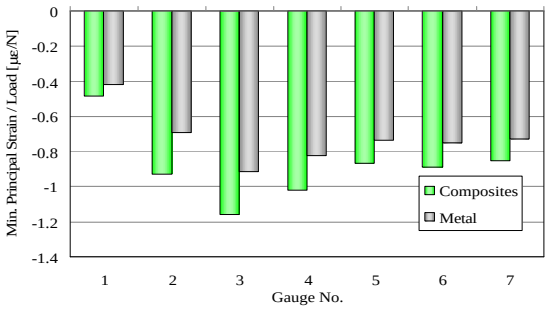

Fig. 25. Minimum principal strain normalized by load on the medial femur

6 Conclusions

A basic design method for composites stem has been proposed and discussed through numerical results of finite element analyses. A Simplified-model which simplifies the shape and the structure of stem and the femur has been proposed for a basic design tool. The modulus of section of Simplified-model is set as same as that of Real-model and mechanical properties are defined by following CT value distributions acquired from some set of CT images. Design parameters are able to be determined qualitatively on a Simplified-model and a Real-model is able to be developed by converting a Simplified-model using linear mapping. It became clear that numerical results of Simplified and Real-model have a good agreement. It is recognized that Simplified-model is a nice tool for basic design of a composites stem and the quantitative determination of design parameters is possible. A flowchart of proposed design procedure is shown in Fig. 26. Furthermore, the advantage of composites stem indicated by numerical results was verified by in-vitro test. It confirmed that composites stem suppresses stress shielding and promotes bone remodeling.

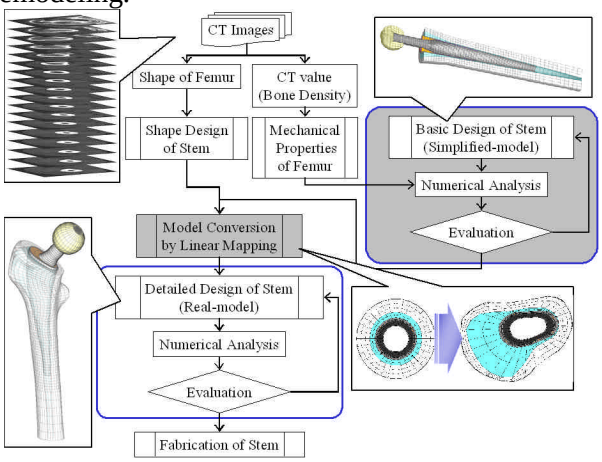

Fig. 26. Flowchart of a design procedure for composites stem based on CT images

Acknowledgements

This study is partially sponsored by the Japan Society for the Promotion of Science (JSPS), "Grant-in-Aid for Scientific Research", category S, subject No. 16100007.

References

[1] World Health Organization 2003 "*Prevention and management of osteoporosis*". Technical Report Series, N0. 921, Iyaku(Medicine and Drug) Journal Co., Ltd., 2005.

[2] Pritchett J. W. "Femoral bone loss following hip replacement. A comparative study". *Clinical Orthopaedics*, Vol. 314, pp 156-161, 1995.

[3] Summer D. R. et al. "Functional adaptation and ingrowth of bone vary as a function of hip implant stiffness". *Journal of Biomechanics*, Vol. 31, pp 909-915, 1998.

[4] Kawamura T., Zako M. et al. "Study on a stiffness design method of femoral prosthesis stem using fiber reinforced composites". *Key Engineering Materials*, Vols. 334-335. pp. 1257-1260, 2007

[5] Zako M. et al. "Development of a design system for total hip replacement by using CT images". *Proceedings of Mechanical Engineering Congress, 2005*, Tokyo, Japan, Vol. 4, 3705, pp. 313-314, 2005.

[6] Sakai T., Sugano N. et al. "Stem length and canal filling in uncemented custom-made total hip arthroplasty". *International Orthopaedics*, Vol. 23, pp. 219-223, 1999.

[7] Nishihara S., Sugano N. et al. "Comparison of the fit and fill between the Anatomic Hip femoral component and the VerSys Taper femoral component using virtual implantation on the ORTHODOC workstation". *Journal of Orthopaedic Science*, Vol. 8, pp. 352-360. 2003.

[8] Vose G. P. and Kubala A. L. "Bone strength – its relationship to X-ray-determined ash content". *Human Biology*, Vol. 31, pp. 261-270, 1959.

[9] Carter D. R. and Hayes W. C. "The compressive behavior of bone as a two-phase porous structure". *Journal of Bone and Joint Surgery*, Vol. 59A, No. 7, pp. 954-962, 1977.

[10] Currey J. D. "The effect of porosity and mineral content on the Young's modulus of elasticity of compact bone". *Journal of Biomechanics*, Vol. 21, pp. 131-139, 1988.

[11] Lotz J. C. Gerhart T. N. and Hayes W. C. "Mechanical properties of metaphyseal bone in the proximal femur". *Journal of Biomechanics*, Vol. 24, pp. 317-329, 1991.

[12] Wirtz D. C. et al. "Critical evaluation of known bone material properties to realize anisotropic FE-simulation of the proximal femur". *Journal of Biomechanics*, Vol. 33, pp. 1325-1330, 2000.

[13] Doblare M., Garcia J. M. and Gomez M. J. "Modeling bone tissue fracture and healing: a review". *Engineering Fracture Mechanics*, Vol. 71, pp. 1809-1840, 2004.

[14] Kalender W. A. "A phantom for standardization and quality control in spinal bone mineral measurement by QCT and DXA: Design considerations and specifications". *Medical Physics*, Vol. 19, No. 3, pp. 583-586, 1992.

[15] Zako M., Takano N., and Tsumura T. "Prediction of Strength for Fibrous Composites based on Damage Mechanics". *Proc. 3rd international symposium TEXCOMP*, Kyoto, Japan, pp. 7/1-7/9, 1996.

[16] Huiskes R. et al. "Adaptive bone-remodeling theory applied to prosthetic-design analysis". *Journal of Biomechanics*, Vol. 20, pp. 1135-1150, 1987.

[17] Weinans H. et al. "Sensitivity of periprosthetic stress-shielding to load and the bone density modulus relationship in subject-specific finite element models". *Journal of Biomechanics*, Vol. 33, pp. 809-817, 2000.

[18] Tai C. L. et al. "Finite Element Analysis of the Cervico-Trochanteric Stemless Femoral Prosthesis". *Clinical Biomechanics*, Vol. 18, pp. 53-58, 2003.

[19] Cristofolini L. "A Critical Analysis of Stress Shielding Evaluation of Hip Prosthesis". *Clinical Review of Biomedical Engineering*, Vol. 25, pp. 409-483, 1997.